

Modeling and Analysis of Three Components of Cutting Force During the Turning of Red Brass (C23000) Using Regression Analysis

Rahul Kshetri, Dr. Ajay

(Department of Industrial & Production Engineering, G.B. Pant University of Agriculture & Technology
Pantnagar- 263145, India)

Corresponding author : Rahul Kshetri

Abstract : In this work an attempt has been made to investigate the effect of input cutting parameters (Cutting speed, feed rate and depth of cut) on cutting forces (feed force, thrust force and cutting force). Experimental values have been compared to the values calculated by regression equation, and surface plots, interaction plots and mean effect plots are drawn for all cutting force component. The results obtained in this study shows that while machining to the red brass (C23000) the depth of cut found the more dominant contributor through all component of cutting forces. With the help of Regression model surface plots are drawn, all interaction on surface for different parameters and their main effects in to all input parameters have also been discussed in this work.

Keywords -Machining by turning, Components of cutting forces, Regression analysis

Date of Submission: 02-06-2018

Date of acceptance: 18-06-2018

I. INTRODUCTION

In a turning operation determination of components of cutting force are important for the design of machine tools. During the operation the machine tool and its components must be able to withstand these forces without causing significant deflections, chatter or vibrations. In turning operation tool cuts unwanted material from the work piece and it experiences a cutting force which can be resolved into three components major force is cutting force along the Y direction, force in Z direction is less in magnitude due to feed this force is also known as feed force, force acts in X direction generally lowest in magnitude for positive rake has the major effect on the accuracy of the job also known as radial force (component of thrust force). Direction of thrust force F_x must acts along the orthogonal plane these forces are shown in **Fig (1)**.

According to review done by researchers it is concluded that, the effect of all three components of force is highly influenced by the geometry of tool (angles and nose radius) including approach angle. **Fig (3)** represents approach angle (χ), direction of feed, direction of rotation (n) and doc during turning. As soon as the cutting angle (Approach angle) increases the value of thrust force decreases, when it reaches at 90° as shown in **Fig (2)** the component of thrust force overlap into the feed force and now only two components of force act on the tool these are feed force (F_z) and main cutting force (F_y).

For cutting tool with positive rake and 90° approach angle, contribution of thrust force is lowest in magnitude whereas cutting force is maximum. For negative rake the largest one force among the force components is thrust force. For rake angle -60° and approach angle 90° magnitude of thrust force is maximum and then cutting force and least magnitude feed force have been occurred [1]. Mustafa Gunay et al.[2] concluded that main cutting force can reduced by increasing rake angle and was increased by increasing value of negative rake angle. Small depth of cut and large negative rake angle is the major cause of this effect [3–5]. Meng Liu et al.[6] studied the effect of nose radius during turning and observed that tool nose radius leads to an increase of the thrust force greatly. Khaider et al.[7] performed experiment in which tool rake angle (-60°) and cutting edge angle 75° have been taken by the author in which contribution of thrust force is maximum in magnitude and contribution of feed force was minimum on turning ASIS bearing steel with CBN tool. Caprino et al. [8] concluded both forces horizontal and vertical undergo large variations with tool wear. Alajmi and Alfares [9] presented a cutting forces prediction model, using back propagation (BP) neural network with an enhancement by differential evolution (DE) algorithm. In this study cutting forces prediction was modeled. Nakayama et al. [10] observed that the higher value of thrust force is the main cause of elastic deformation of cutting zone which one is the key cause of dimensional error on machined work piece. Lima et al. [11] studied the effects of cutting speed, feed rate and depth of cut on surface roughness and cutting forces for AISI 4340 high strength low alloy steel and AISI D2 cold work tool steel materials. Chou and Song [12] reported that rake angle (-25°) with a large nose radius enhanced the value of force components which is helpful for batter surface finishing during

hard turning of AISI 52100 steel with ceramic tool. Another explanation made by Astakhov [13] he bound up the dominance of thrust force to the spring back of the machined surface. Bouacha et al. [14] investigate to thrust force evolution and concluded that the hardness of work pieces is a function of thrust force Kurt and Seker [15] studied and concluded that the thrust force has to be influences by the chamfer angle of PCBN insert as compared to tangential component. Ultimately the conclusion has been drawn that is at low cutting speed magnitude of force would be high and must be the formation of built up edge that would be the cause of increases in dynamic forces and excessive chipping now due to excessive chipping tool failure occurs [16]. Similarly, cutting force components decrease with high cutting speed and is causes decreasing shear force value hence there effect can easily shown because of low enhancement in temperature and there who reduces the formation of built up edge. The S.K. Birla et al [17] studied that cutting force affected by many parameters in steady state conditions and the variation of cutting force with time has a peculiar characteristic. Bagawade et al. [18] studied that cutting speed and depth of cut is more responsible causes of force components as compared to feed rate Bouacha et al. [19] performed the experiment and concluded that cutting speed is more influential parameter for thrust force and In finish hard turning, component of thrust force usually the largest in magnitude, the middle one is tangential cutting force and the is the smallest is feed force. Assumption is that feed rate, cutting speed, and depth of cut plays significance effects for cutting force components experiment had performed for, AISI 52100 steel hard turning with CBN tool. I. Meddour et al [20] studied that with increasing depth of cut thrust force increases and reaches there maximum value for feed 0.14 mm/rev. And after that by increasing depth of cut thrust force decreases, hard turning of AISI 52100 steel. Sundaram and Lambert [21] studied the effect of cutting time, feed, speed, depth of cut, and tool coating and to develop mathematical model multiple regression technique has been used.

M. Hanief et al [22] developed a predictive mathematical model for turning operation on red brass(C23000) using ANN and regression analysis now presented model is capable for determining the value of cutting forces. It is concluded that with increase of feed, speed and depth of cut value of cutting force increases. Contribution of feed rate is maximum for resultant force component whereas the least contribution occurs due to depth of cut.

The presented work includes development of mathematical models independently for three components of force experienced by the cutting tool during turning of material C23000 brass alloy. Experimental data given in the work is used for this purpose. [22]

UNS C23000 brass alloys are used for cold formed hardware, jewelry and electrical components, fittings, decorative chains and dezincification resistant fasteners.

II. METHODOLOGY

Regression analysis is used to do the mathematical modeling of each of three components of cutting force. Minitab is use for this purpose. Experimental data mentioned in **Table (1)** [22] is used for generate mathematical models.

$$F_r(N) = 4.3 + 0.0129 * V + 13.81 * f - 166 * d - 0.000005 * V * V - 8.15 * f * f + 696 * d * d - 0.00082 * V * f - 0.0019 * V * d + 11.2 * f * d \dots\dots\dots(1)$$

New regression model equation for resultant force is given by **Equation (1)**

Percentage error between previous existing and new developed model is very low, so now the new mathematical model is acceptable for each cutting parameters. Comparison between both model have been clearly shown in **Fig (4)**.

As per the result of graph drawn in between previous and presented model and their error analysis it has been clear that methodology of new developed model is accurate. Now same methodology is being recommended for analysis of other components of forces. Surface plots for resultant force are shown in **Fig (5)**, Interaction plots for resultant force for cutting speed, feed rate and doc are shown in **Fig (6)**, and main effect plots of resultant cutting forces are shown in **Fig (7)**.

Model equation for thrust force 'Fx (N)' is given by **Equation (2)**.

$$F_x(N) = -1.0 + 0.0107 * V + 12.23 * f - 68 * d - 0.000007 * V * V - 7.98 * f * f + 126 * d * d - 0.00092 * V * f + 0.0376 * V * d - 16.2 * f * d \dots\dots\dots(2)$$

Surface plots for thrust force component for different cutting parameters are shown in **Fig (8)**, interaction plots for thrust force are shown in **Fig (9)** and main effect plots for thrust force are shown in **Fig (10)**.

Model equation for cutting force component is given by **Equation (3)**.

$$F_y(N) = 6.24 + 0.0005 * V + 9.44 * f - 111.9 * d + 0.000001 * V * V - 5.23 * f * f + 560 * d * d + 0.00058 * V * f - 0.0210 * V * d + 20.6 * f * d \dots\dots\dots(3)$$

Surface plots of cutting force component for varying cutting speed feed rate and doc are shown in **Fig (11)**. Interaction plots for cutting force component and Main effect plots are shown in **Fig.(12-13)**

Model equation for feed force is given by **Equation (4)**

$$F_z(N) = 0.2 + 0.0139 * V + 8.09 * f - 106.5 * d - 0.000006 * V * V - 5.58 * f * f + 446 * d * d - 0.00102 * v * f + 0.0020 * V * d - 12.8 * f * d \dots\dots\dots(4)$$

Surface plots, interaction and main effect plots are shown in **Fig (14-16)**.

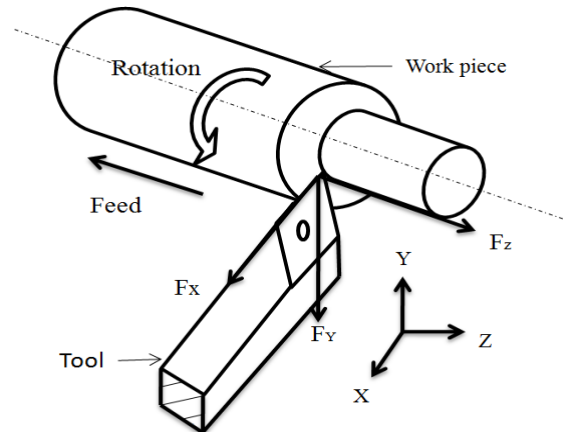


Fig (1) Component of Forces during Turning

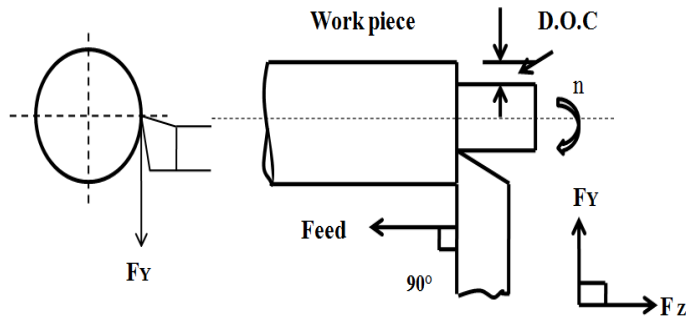


Fig (2) External turning with approach angle ($\chi = 90^\circ$)

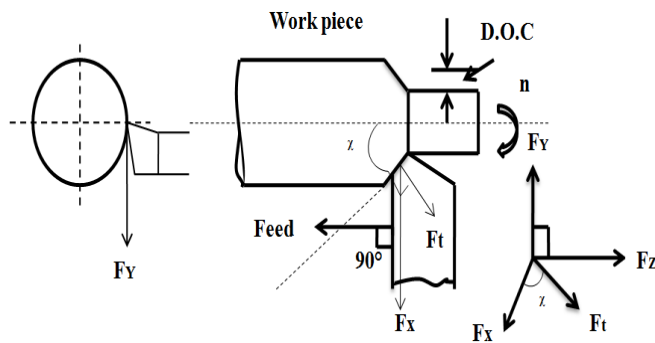


Fig (3) External turning with approach angle ($\chi \neq 90^\circ$)

Table (1) Experimental and model generated data

Speed (m/min)	Feed (mm/rev)	Depth of cut (mm)	Thrust Force (F _x) (N)	Cutting Force (F _y) (N)	Feed Force (F _z) (N)	Resultant force (F _R) (N)	Existing model Fe(N)	New Generated Model Fn(N)	% Error
840	0.4	0.1	1.864	4.231	2.215	5.126	5.988	6.200	3.551
840	0.4	0.13	1.994	4.122	3.651	5.856	6.479	6.109	5.712
840	0.4	0.16	3.194	5.320	3.977	7.370	6.897	7.271	5.421
1280	0.4	0.1	2.374	4.779	3.277	6.263	6.576	6.984	6.205
1280	0.4	0.13	4.012	5.020	4.528	7.861	7.116	6.868	3.486
1280	0.4	0.16	3.944	6.443	5.009	9.065	7.575	8.005	5.673
1000	0.4	0.1	3.492	4.281	3.76	6.683	6.225	6.71	7.787
1000	0.4	0.13	3.612	5.056	3.16	6.971	6.736	6.609	1.879
1000	0.4	0.16	4.035	5.831	3.189	7.775	7.170	7.762	8.253
840	0.8	0.1	3.863	6.342	3.152	8.067	7.981	7.985	0.050
840	0.8	0.13	2.522	7.734	2.128	8.408	8.636	8.028	7.040
840	0.8	0.16	2.811	9.117	3.093	10.029	9.193	9.324	1.429
1280	0.8	0.1	2.464	7.663	2.944	8.571	8.765	8.625	1.605
1280	0.8	0.13	3.126	7.449	2.692	8.516	9.485	8.643	8.880
1280	0.8	0.16	2.756	8.806	3.752	9.961	10.097	9.914	1.808
1000	0.8	0.1	4.349	6.766	3.825	8.907	8.297	8.442	1.745
1000	0.8	0.13	3.349	6.766	3.825	8.907	8.978	8.476	5.594
1000	0.8	0.16	1.788	7.6812	2.560	8.291	9.557	9.763	2.155
840	0.12	0.1	2.810	1.6157	2.462	4.071	3.635	3.399	6.478
840	0.12	0.13	1.812	1.631	2.287	3.343	3.934	3.214	18.281
840	0.12	0.16	1.203	2.726	2.755	4.059	4.187	4.282	2.265
1280	0.12	0.1	2.161	2.505	4.247	5.384	3.992	4.285	7.318
1280	0.12	0.13	1.341	1.245	1.568	2.410	4.320	4.074	5.691
1280	0.12	0.16	1.665	2.821	3.426	4.855	4.599	5.117	11.267
1000	0.12	0.1	1.734	2.091	2.847	3.935	3.779	3.945	4.404
1000	0.12	0.13	1.362	2.376	2.854	3.955	4.089	3.751	8.268
1000	0.12	0.16	1.7977	2.851	4.11	5.315	4.353	4.810	10.492

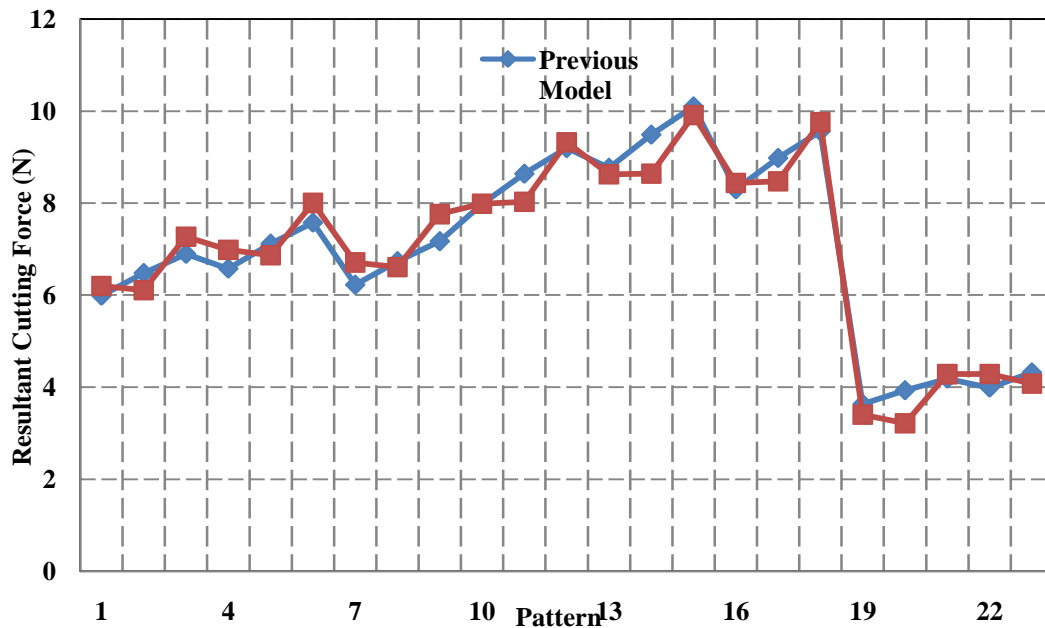


Fig (4) Comparison on resultant force of previous and new developed model

Surface Plots of Fr (N)

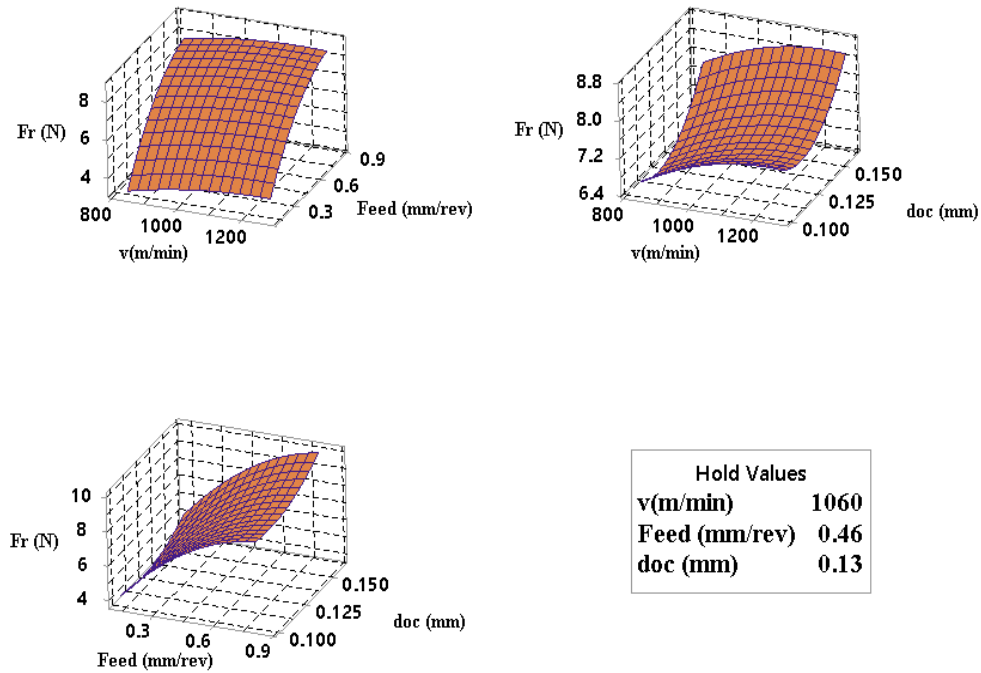


Fig (5) Surface plotes of Resultant force for varying cutting speed ,feed rate and doc

Interaction Plot for Fr (N) Fitted Means

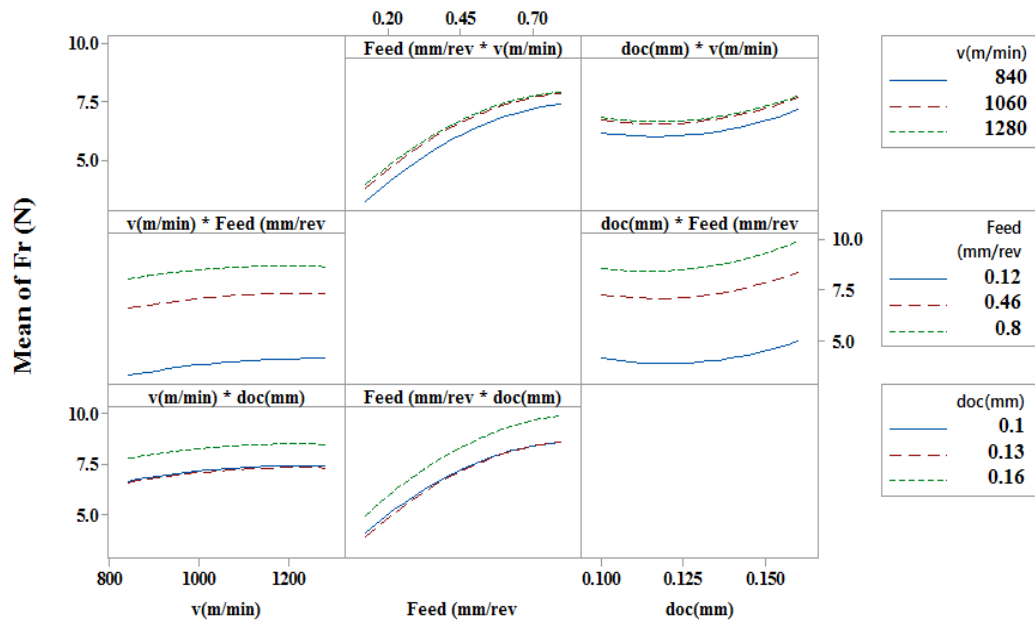


Fig (6) Interaction plots for resultant force

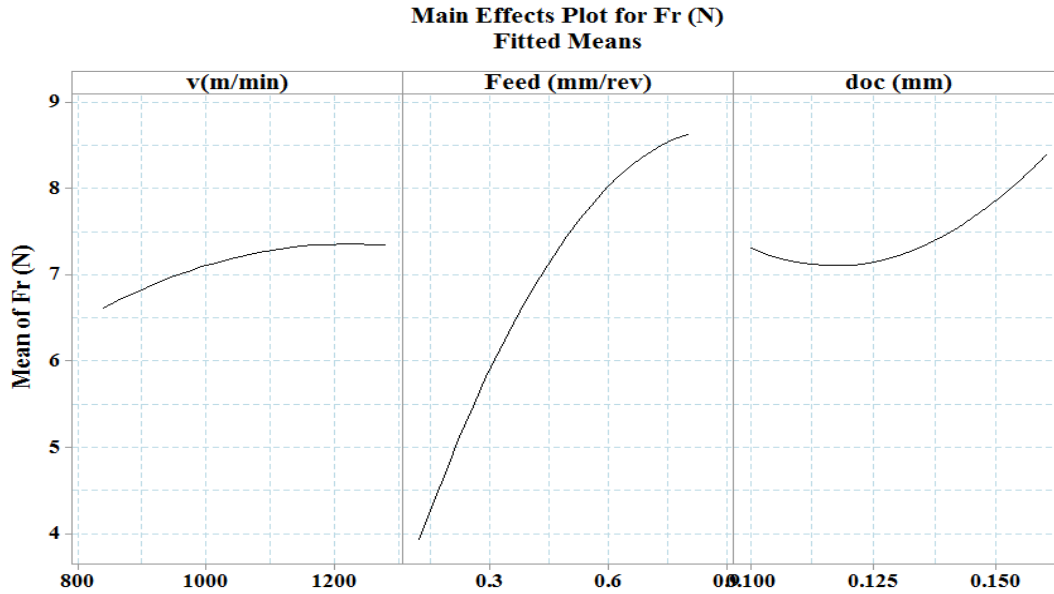


Fig (7) Main effects of cutting speed, feed rate and doc on resultant force

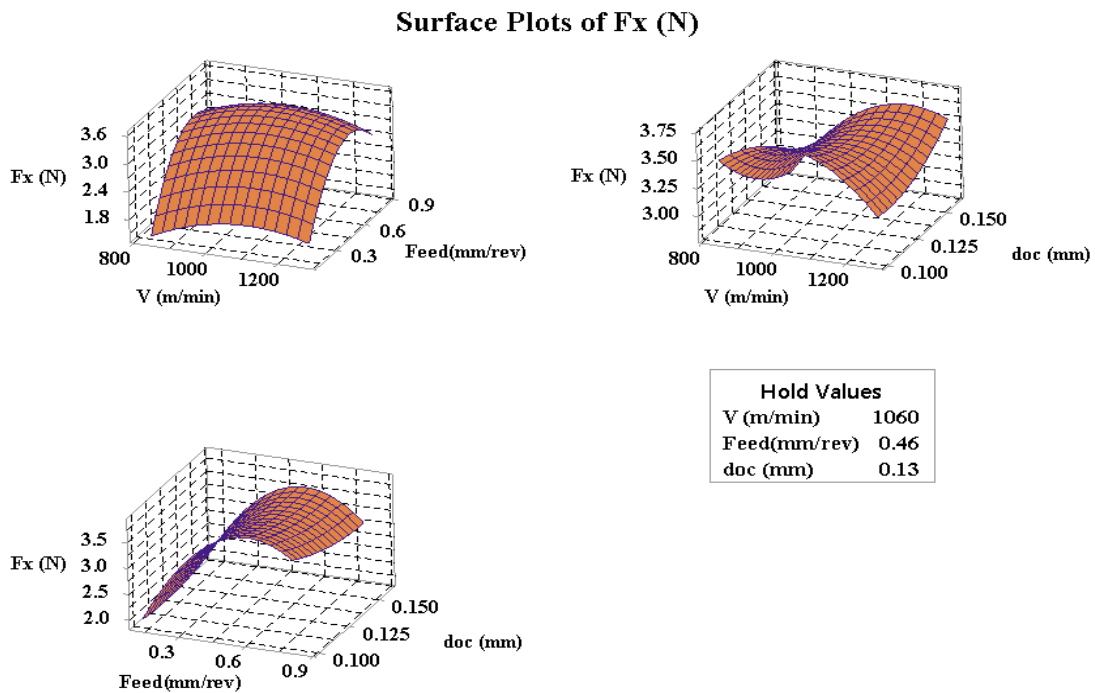


Fig (8) Surface plots for thrust force with varying cutting parameters

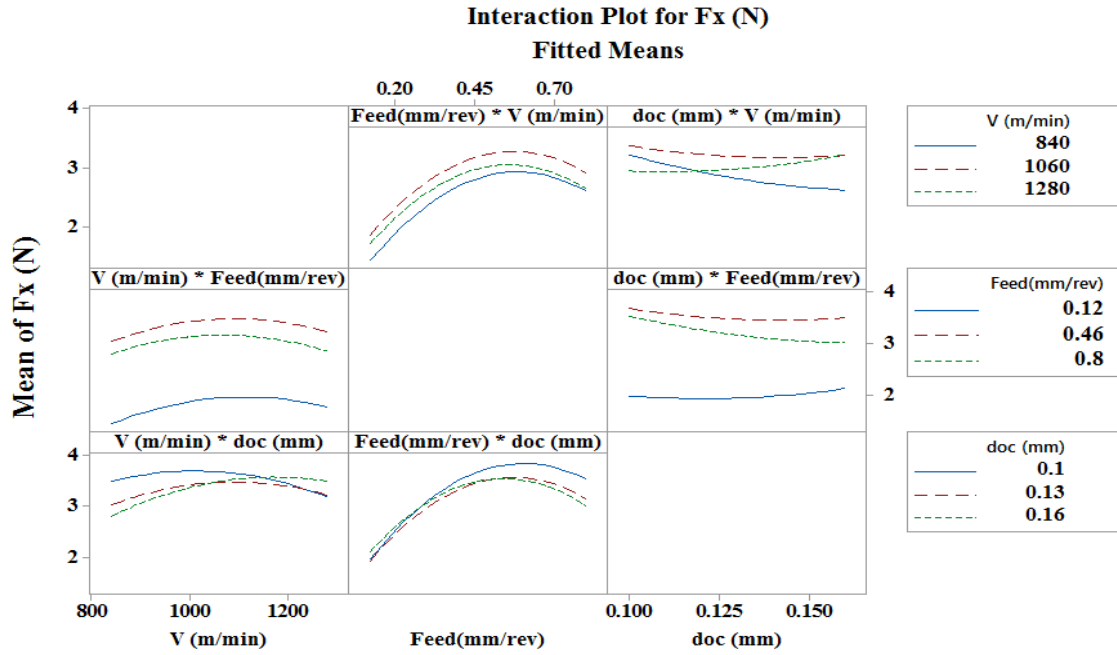


Fig (9) Interaction plots for thrust force component

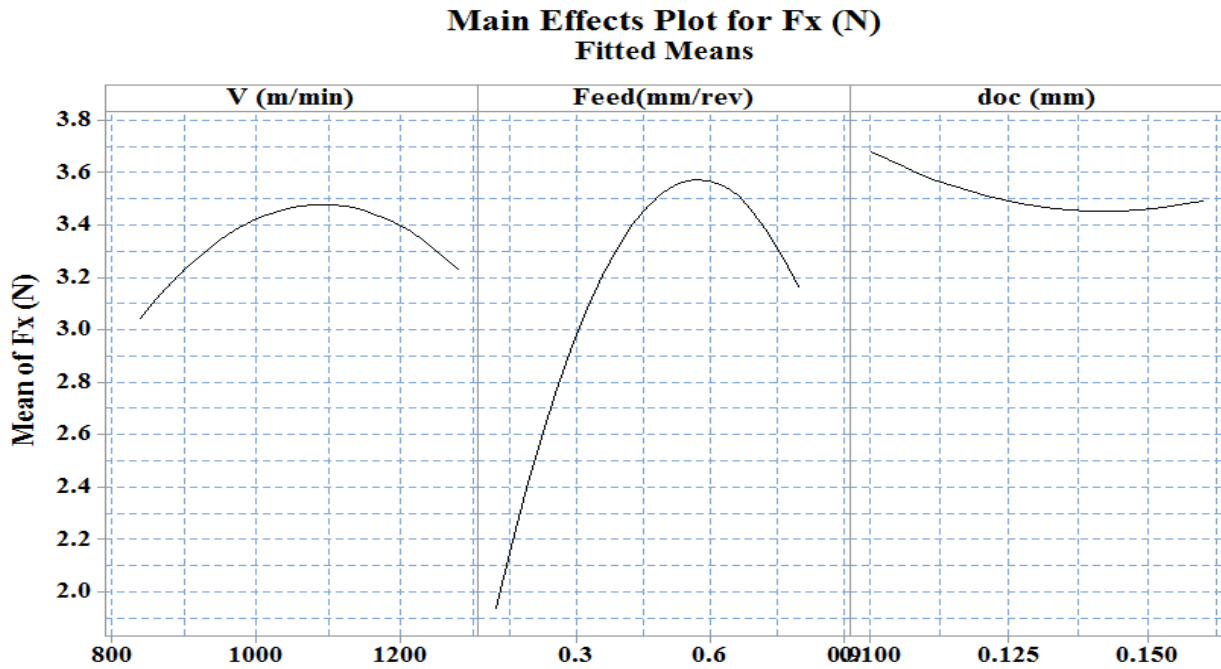


Fig (10) Main effect plots for thrust force with varying cutting parameters

Surface Plots of Fy (N)

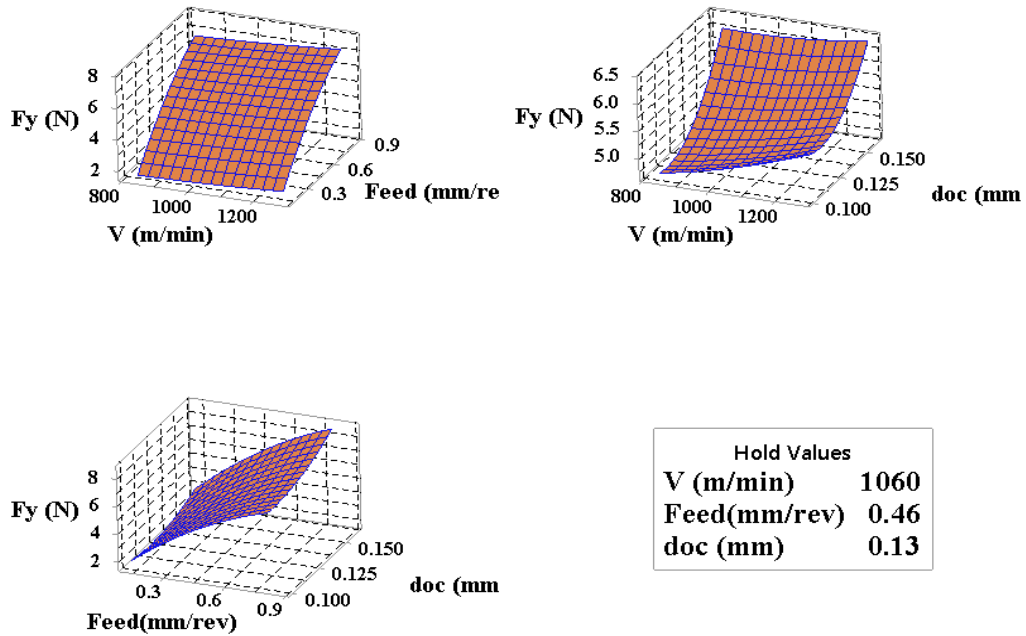


Fig (11) Surface plots for cutting force component for varying cutting parameters

Interaction Plot for Fy (N)
Fitted Means

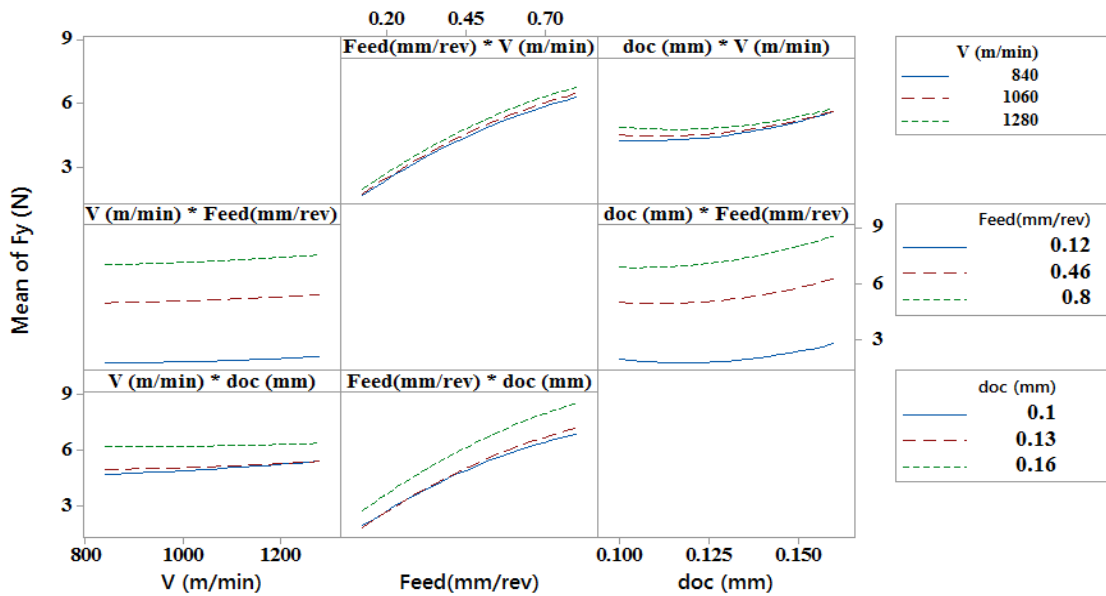


Fig (12) Interaction plots of cutting force component for varying cutting parameters

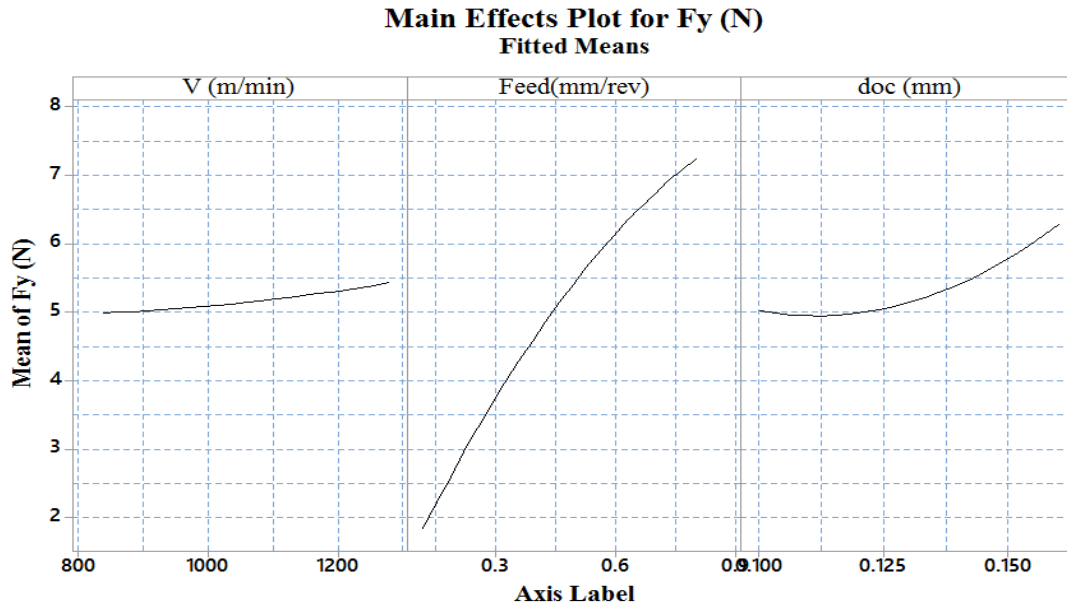


Fig (13) Main effect plots for varying cutting parameters

Surface Plots of F_z (N)

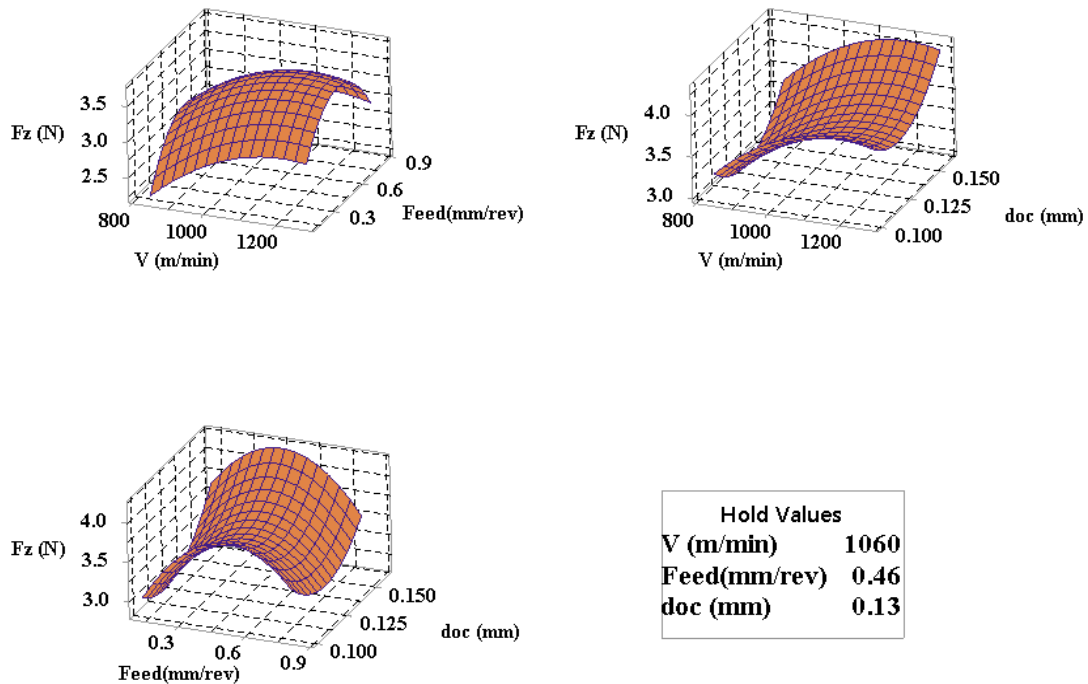


Fig (14) Surface plots for thrust force component with varying cutting parameters

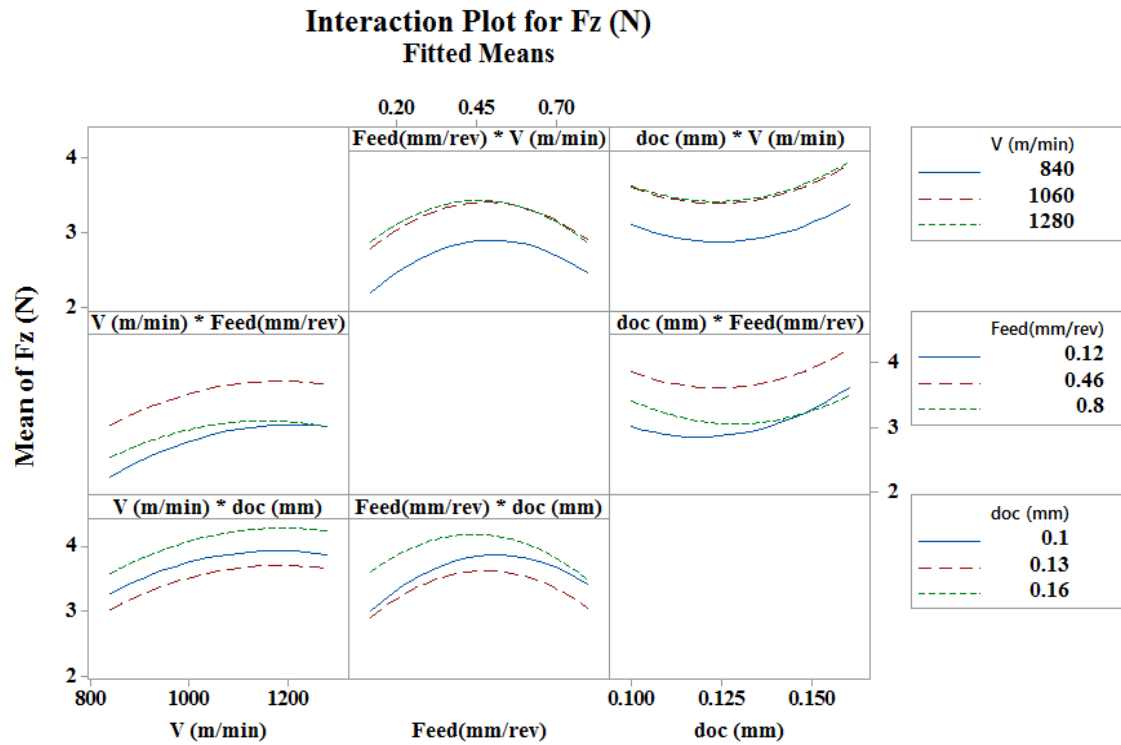


Fig (15) Interaction plots for feed force component with varying cutting parameter

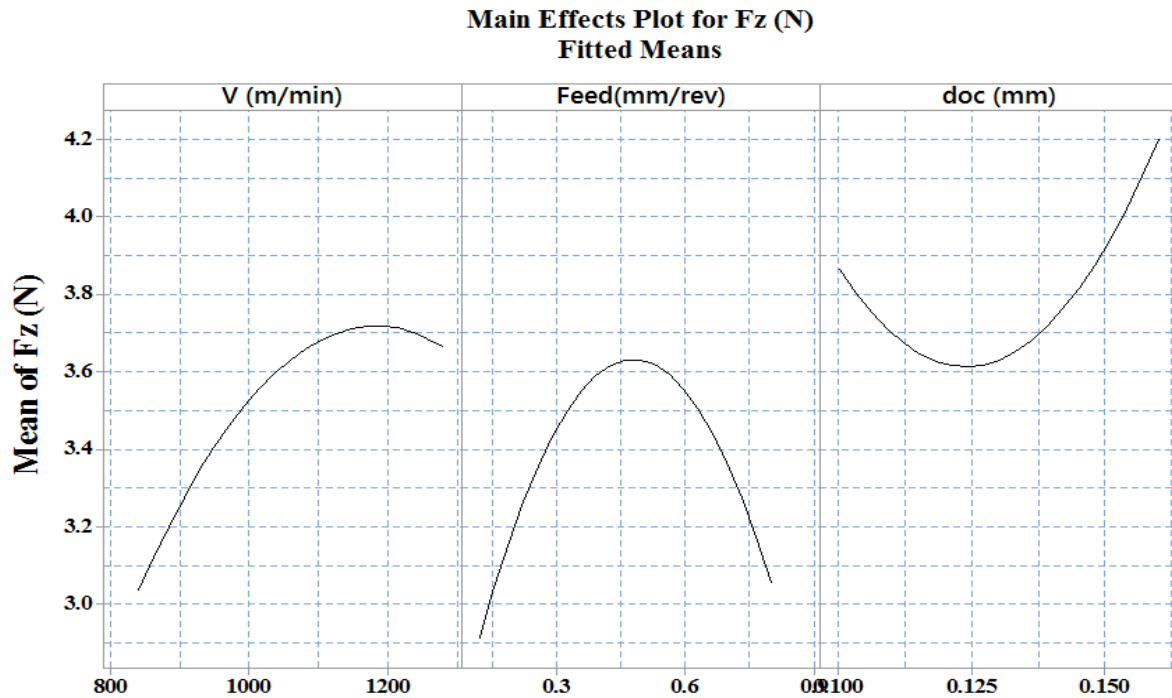


Fig (16) Main effect plot for feed force with varying cutting parameters

III. CONCLUSION

Percentage error of resultant force in between new generated model (Presented model that is developed by regression equation) and experimental model is an acceptable limit that has been shown in Fig.4. Now surface plots of different models based on regression model concludes following conclusions.

- Resultant force increases with increasing speed and reaches maximum value at 1200m/min and then decreases with increasing speed.
- As soon as feed rate and doc increasing resultant force also increases.
- Component of thrust force first increases and then decreased with increasing speed; at 1100m/min it reaches maximum value.
- With increasing feed rate component of thrust force increases, where as doc first decreasing (minimum value found when doc 0.127mm) and then increased.
- Cutting force component first increasing with speed and then decreasing.
- With increasing feed rate and doc cutting force increases.
- Feed force component is maximum at 1150 m/min cutting speed and then decreasing.
- With increasing feed rate feed force component increases, at cutting speed 0.5 mm/rev feed force component obtained its maximum value and then decreasing.

REFERENCES

- [1]. Lalwani, D. I., N. K. Mehta, and P. K. Jain. "Experimental investigations of cutting parameters influence on cutting forces and surface roughness in finish hard turning of MDN250 steel." *Journal of materials processing technology* 206.1 (2008): 167-179.
- [2]. Günay, Mustafa, et al. "Experimental investigation of the effect of cutting tool rake angle on main cutting force." *Journal of materials processing technology* 166.1 (2005): 44-49.
- [3]. Manufacturing Science by Amitabh Ghosh Ashok Kumar Mallik ,page no (191-199).
- [4]. Meng L, Jun-ichiro T, Akira T (2004) Effect of tool nose radius and tool wear on residual stress distribution in hard turning of bearing steel. *J Mater Process Technol* 150:234–241
- [5]. Yallesc MA, Chaoui K, Zeghib N, Boulanouar L, Rigal J (2009) Hardmachining of hardened bearing steel using cubic boron nitride tool. *J Mater Process Technol* 209:1092–1104
- [6]. Liu, Meng, Jun-ichiro Takagi, and Akira Tsukuda. "Effect of tool nose radius and tool wear on residual stress distribution in hard turning of bearing steel." *Journal of Materials Processing Technology* 150.3 (2004): 234-241.
- [7]. Bouacha, Khaider, et al. "Statistical analysis of surface roughness and cutting forces using response surface methodology in hard turning of AISI 52100 bearing steel with CBN tool." *International Journal of Refractory Metals and Hard Materials* 28.3 (2010): 349-361.
- [8]. G. Caprino, I. De Lorio, L. Nele, L. Santo, Effect of tool wear on cutting forces in orthogonal cutting of unidirectional glass fiber reinforced plastics, *Composites Part A* 27A (1996) 409–415.
- [9]. Alajmi, M. S., & Alfares, F. (2007). Prediction of cutting forces in turning process using De-Neural Networks. *Artificial Intelligence and Applications, AIA 2007, 2/12/2007–2/14/2007, Innsbruck, Austria*
- [10]. Nakayama K, Arai M, Kanda T (1988) Machining characteristic of hard materials. *CIRP Ann Manuf Technol* 37:89–92
- [11]. J.G. Lima, R.F. Avila, A.M. Abrão, M. Faustino, J.P. Davim, Hard turning: AISI 4340 high strength low steel and AISI D2 cold work tool steel, *J Mater Process Technol* 169 (2005) 388–395
- [12]. Chou YK, Song H (2004) Tool nose radius effects on finish hard turning. *J Mater Process Technol* 148(2):259–268
- [13]. Astakhov VP (2010) *Geometry of single-point turning tools and drills. Fundamentals and practical applications.* Springer, London
- [14]. Bouacha K, Yallesc MA, Mabrouki T, Rigal J (2010) Statistical analysis of surface roughness and cutting forces using response surface methodology in hard turning of AISI 52100 bearing steel with CBN tool. *J Refract Met Hard Mater* 28:349–361
- [15]. Kurt A, Seker U (2005) The effect of chamfer angle of polycrystalline cubic boron nitride cutting tool on the cutting forces and the tool stresses in finishing hard turning of AISI 52100 steel. *Mater Des* 26:351–356
- [16]. Aslan E, Camuscu N, Birgoren B (2007) Design optimization of cutting parameters when turning hardened AISI 4140 steel (63 HRC) with Al₂O₃ + TiCN mixed ceramic tool. *Mater Des* 28:1618–1622
- [17]. S.K. Birla, Sensors for adaptive control and machine diagnostics, *Proc. Mach. Tool Task Force Conf.*, vol. 4, 1980, pp. 7–12.
- [18]. Bagawade AD, Ramdasi PG, Pawade RS, Bramhankar PK (2012) Evaluation of cutting forces in hard turning of AISI 52100 steel by using Taguchi method. *J Eng Res Technol* 1(6):2278–0181
- [19]. Bouacha K, Yallesc MA, Mabrouki T, Rigal J (2010) Statistical analysis of surface roughness and cutting forces using response surface methodology in hard turning of AISI 52100 bearing steel with CBN tool. *J Refract Met Hard Mater* 28:349–361
- [20]. Meddour, I., et al. "Investigation and modeling of cutting forces and surface roughness when hard turning of AISI 52100 steel with mixed ceramic tool: cutting conditions optimization." *The International Journal of Advanced Manufacturing Technology* 77.5-8 (2015): 1387-1399.
- [21]. R.M. Sundaram, B.K. Lambert, Mathematical models to predict surface finish in fine turning of steel, *Int. J. Prod. Res. (Parts 1 and 2)* 19 (1981) 547–564
- [22]. Hanief, M., M. F. Wani, and M. S. Charoo. "Modeling and prediction of cutting forces during the turning of red brass (C23000) using ANN and regression analysis." *Engineering Science and Technology, an International Journal* (2016).

Rahul Kshetri "Modeling and Analysis of Three Components of Cutting Force During the Turning of Red Brass (C23000) Using Regression Analysis" *International Journal of Engineering Science Invention (IJESI)*, vol. 07, no. 06, 2018, pp 69-79